The Biodistribution and Radiation Dosimetry of the Arg-Gly-Asp Peptide ^{18}F-AH111585 in Healthy Volunteers

Brian J. McParland[1,2], Matthew P. Miller[1], Terence J. Spinks[3], Laura M. Kenny[4], Safiye Osman[3], Mandeep K. Khela[1], Eric Aboagye[4], Raoul C. Coombes[4], Ai-Min Hui[1], and Pamela S. Cohen[1]

[1]Research and Development, Medical Diagnostics, GE Healthcare Ltd., Amersham, Buckinghamshire, England; [2]Global Imaging Network, GE Healthcare Medical Diagnostics, Grove Centre, Amersham, Buckinghamshire, England; [3]Hammersmith Imanet Ltd., Hammersmith Hospital, London, England; and [4]Department of Oncology, Imperial College Faculty of Medicine, Hammersmith Hospital, London, England

We report the safety, biodistribution, and internal radiation dosimetry of a new PET tracer, ^{18}F-AH111585, a peptide with a high affinity for the $\alpha_v\beta_3$ integrin receptor involved in angiogenesis. **Methods:** PET scans of 8 healthy volunteers were acquired at time points up to 4 h after a bolus injection of ^{18}F-AH111585. ^{18}F activity in whole blood and plasma and excreted urine were measured up to 4 h after injection. In vivo ^{18}F activities in up to 12 source regions were determined from quantitative analysis of the images. The cumulated activities subsequently calculated were then used to determine the internal radiation dosimetry, including the effective dose. **Results:** Injection of ^{18}F-AH111585 was well tolerated in all subjects, with no serious or drug-related adverse events reported. The main route of ^{18}F excretion was renal (37%), and the 3 highest initial uptakes were by liver (15%); combined walls of the small, upper large, and lower large intestines (11%); and kidneys (9%). The 3 highest absorbed doses were received by the urinary bladder wall (124 μGy/MBq), kidneys (102 μGy/MBq), and cardiac wall (59 μGy/MBq). The effective dose was 26 μGy/MBq. **Conclusion:** ^{18}F-AH111585 is a safe PET tracer with a dosimetry profile comparable to other common ^{18}F PET tracers.

Key Words: ^{18}F-AH111585; $\alpha_v\beta_3$ expression; PET; dosimetry; whole-body biodistribution

J Nucl Med 2008; 49:1664–1667
DOI: 10.2967/jnumed.108.052126

Integrin receptors are heterodimeric transmembrane proteins, expressed on the surfaces of endothelial cells and by a variety of tumor types, that bind to neighboring cell membrane proteins and the extracellular matrix (*1,2*). In particular, $\alpha_v\beta_3$ integrin receptors are associated with the regulation of tumor growth and are expressed on activated endothelial cells. As $\alpha_v\beta_3$ receptor antagonists are being evaluated for antiangiogenic therapy (*3*), clear interest in developing means of in vivo monitoring of such therapy is evident. Several molecular imaging agents have been investigated for the provision of in vivo assessment of angiogenesis (*4,5*).

AH111585 is a cyclic peptide containing an arginine-glycine-aspartic acid (RGD) motif that binds to integrin receptors such as $\alpha_v\beta_3$ with high affinity. We are investigating ^{18}F-labeled AH111585 for the quantitative in vivo monitoring of antiangiogenic therapy using PET. Details of the ^{18}F-AH111585 agent and its feasibility in detecting primary and metastatic cancer have been described previously (*6*). The study described here determined the safety of ^{18}F-AH111585 in healthy adult volunteers, biodistribution of ^{18}F, and the associated radiation dosimetry calculated after the MIRD schema (*7*).

MATERIALS AND METHODS

Unless otherwise specified, numeric data are provided as the mean ± 1 SD.

Radiopharmaceutical Preparation

Synthesis of the agent has been described previously (*6,8*).

Subjects

Approval for this study was received from the Hammersmith Hospitals NHS Trust Research Ethics Committee, the Administration of Radioactive Substances Advisory Committee, and the Medicines and Healthcare Products Regulatory Agency. Eight healthy volunteers (5 men, 3 women), with an age of 61 ± 4 y and body mass index of 27.2 ± 2.8 kg/m^2, were recruited. Inclusion criteria included age between 50 and 65 y, ability to provide informed written consent, and normal medical history (including physical examination, electrocardiogram, hematology, and biochemistry). Exclusion criteria included pregnancy and lactation.

Safety

Safety data collected up to 72 h after injection included adverse events (AEs); vital signs (blood pressure, respiratory rate, heart rate,

Received Mar. 31, 2008; revision accepted Jun. 26, 2008.
For correspondence or reprints contact: Brian J. McParland, Global Imaging Network, GE Healthcare Medical Diagnostics, Grove Centre GC/58, White Lion Rd., Amersham, Buckinghamshire, England HP7 9LL.
E-mail: brian.mcparland@ge.com

and body temperature); physical examination; cardiovascular, lung, abdomen, and neurologic examinations; electrocardiogram; and laboratory parameters (serum biochemistry, hematology, coagulation, and urinalysis). Blood samples were collected through an indwelling catheter, and to avoid occlusion, heparinized saline was used for line flushing.

Image Acquisition and In Vivo Activity Measurement

Images were acquired with a 962 EXACT HR+ PET scanner (CTI/Siemens) with 15.5-cm axial and 58-cm transaxial fields of view. Before administration of ^{18}F-AH111585, a transmission scan of each subject was performed using ^{68}Ge sources to provide attenuation maps. A whole-torso emission scan consisted of contiguous static images acquired at 6 bed positions, with the inferior border set to include the urinary bladder within the field of view and the superior border set at approximately the level of the epiglottis or above. The total axial length of the concatenated image was 81 cm, and ^{18}F activity in the anatomy outside the field of view (part of the head and lower extremities) was assumed uniformly distributed and equal to the difference between that administered and measured in the imaged anatomy.

The mean injected ^{18}F activity in the subjects was 163.7 MBq (range, 155.2–173.1 MBq) via an antecubital vein. The mean administered AH111585 mass dose was 2.5 μg (range, 1–4.5 μg), and the mean injected volume was 3.3 mL (range, 2–5.5 mL) for a specific activity of 147 GBq/μmol (range, 69–292 GBq/μmol). Three-dimensional whole-torso acquisitions of subjects were taken at 4 time points up to 4 h after injection with nominal start times of 5, 50, 100, and 160 min after injection. To compensate for physical decay of ^{18}F, the acquisition for each bed position increased 4, 5, 6, and 7.5 min per individual bed position for these 4 time points after injection.

Emission data were reconstructed using the ordered-subsets expectation maximization (OSEM) algorithm (6 iterations and 16 subsets) (*9*) and filtered backprojection (FBP) (*10*). Whereas OSEM-reconstructed tomographic images provided superior delineation, enabling definition of anatomic regions of interest (ROIs), phantom measurements demonstrated that FBP-reconstructed images provided more accurate quantification of ^{18}F activity. Hence, ROIs were defined on OSEM-reconstructed images and mapped to the corresponding FBP image to extract the ^{18}F activities using ANALYZE analysis software (version 7; Biomedical Imaging Resource, Mayo Clinic). Coronal reconstruction was used, and 256 slices for each reconstructed set were collapsed to a single plane and ROIs drawn around specific visible organs and any other structures displaying uptake. ^{18}F activities were decay-corrected to the time of injection and normalized to the total administered activity.

ROIs included salivary glands, thyroid, lungs, heart, liver, gallbladder, spleen, gastrointestinal tract, kidneys, urinary bladder contents, and remaining tissues. The gastrointestinal tract demonstrated rapid nonspecific uptake by soft tissue that cleared while activity within the gastrointestinal tract contents was introduced through hepatobiliary drainage. To isolate both contributions, an ROI was placed over the quadriceps femoris muscle, and ^{18}F activity washout was measured. This time–activity curve was rescaled to that of the gastrointestinal tract ROI at the first imaging time, when there was no activity in the gastrointestinal tract contents, and the result was subtracted from the total gastrointestinal tract ROI activity at subsequent time points to yield ^{18}F activity within the gastrointestinal tract contents alone.

Measurement of In Vitro Activity

Venous blood samples were taken at nominal times of 5, 10, 15, 30, 60, 90, 150, and 240 min after injection. Dual 1-mL aliquots each of whole blood and plasma were obtained from each sample, and ^{18}F activity concentration was measured in a well counter. Urine was collected as voided up to 240 min after injection, and the volume and time of each micturition recorded. Dual 0.1-mL aliquots of urine were sampled from each void, the mean ^{18}F activity per aliquot was measured, and the resulting ^{18}F activity concentration was multiplied by the volume of voided urine to provide the ^{18}F activity excreted.

As the heart wall and blood contained within are MIRD-specified source regions, ^{18}F activity within each region was determined by considering the activity extracted from the heart ROI as the sum of those within the cardiac wall and blood contents. The latter was estimated by the product of the measured ^{18}F activity concentration in whole blood at the time of imaging and the sex-specific reference volumes of cardiac chamber blood (*11*). The measured ^{18}F activity concentration was then subtracted from the activity in the heart ROI to isolate that in the heart wall.

Biodistribution

For each source region, the decay-corrected ^{18}F activity over the 4 time points was least-squares-fit by an analytic function. Physical decay of ^{18}F was incorporated and the function integrated to yield the cumulated activity (numerically equal to the residence time, the cumulated activity normalized to the administered activity is presented here in units of MBq·h/MBq to avoid confusion with temporal quantities). Cumulated activities of the contents of the small intestine, upper large intestine, and the lower large intestine were calculated using a dynamic model for the gastrointestinal tract (*12*) with the assumption that all activity enters the duodenum via hepatobiliary transport. The cumulated activity in the urinary bladder contents and voided urine was calculated using a dynamic urinary bladder model (*13*) for a 3.5-h voiding interval (*14*).

Internal Radiation Dosimetry

The internal radiation dosimetry for the adult human was evaluated through the normalized cumulated activities for each subject provided as input to the OLINDA/EXM code (*15*). The resulting ensemble of mean absorbed doses per unit administered activity was then used to calculate the effective dose per unit administered activity (*16*), with the following modifications: the gonadal dose as the arithmetic mean of the testicular- and ovarian-absorbed doses (*14*); removal of the upper large intestine wall from the remaining organ category and calculation of the colon-absorbed dose as the fractional mass-weighted sum of the mean absorbed doses to the walls of the upper and lower large intestines (*17*); and the thymus-absorbed dose as a surrogate for that to the esophagus (*17*).

The organ-absorbed doses and effective dose evaluated for each individual subject were subsequently averaged.

RESULTS

Unless otherwise specified, all ^{18}F activities are decay-corrected to time of injection and expressed as a percentage of the administered activity.

Safety

^{18}F-AH111585 was found to be safe and well tolerated in all subjects. No serious AEs or drug-related AEs were reported. Two of 8 subjects had a total of 3 non–drug-related

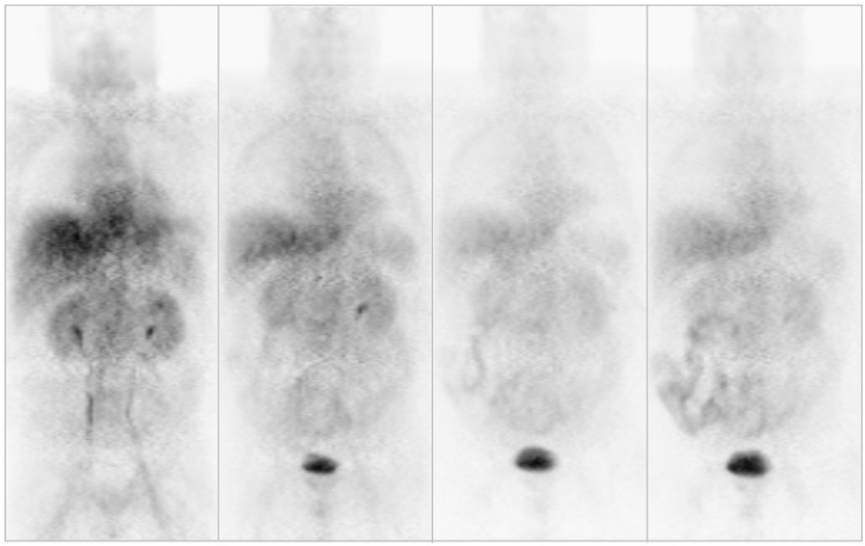

FIGURE 1. Series of whole-torso images of representative subject showing biodistribution of ^{18}F activity for acquisitions begun between 5 and 208 min after administration of ^{18}F-AH111585. p.i. = after administration.

AEs, including catheter site–related reaction, headache, and dyspepsia. No other abnormalities were seen except for increase in activated partial thromboplastin time (aPTT; reference range, 20.4–31.4 s). Transient, asymptomatic increases in aPTT (up to 30.4 s above reference range) after ^{18}F-AH111585 administration were observed in 5 of 8 subjects (62.5%). The increases in aPTT completely reversed within 24 h without any treatment and were likely due to the use of intravenous heparin flushes in the same catheter from which the aPTT samples were drawn. There was no evidence of clinical bleeding.

Biodistribution

Images of a representative male subject between 5 and 208 min after injection of ^{18}F-AH111585 are presented in Figure 1. All subjects demonstrated initially high uptake in the liver, spleen, and heart wall. The mean initial uptake of activity in the liver was 15% ± 5%, with washout decreasing to 8% ± 2% at about 4 h after injection. The estimated ^{18}F activity excreted through the urinary pathway and the gastrointestinal tract were 37% ± 14% and 20% ± 5%, respectively. The biologic half-life of ^{18}F activity in whole blood was 0.25 ± 0.07 h. Table 1 provides the cumulated activities. Source regions with the 3 highest mean normalized cumulated activities (excluding remaining tissues) are those of the combined urinary bladder contents and voided urine (0.456 MBq·h/MBq for a 3.5-h voiding interval), liver (0.23 MBq·h/MBq), and gastrointestinal tract wall (0.22 MBq·h/MBq).

Radiation Dosimetry

Table 2 summarizes the organ- or tissue-absorbed doses. Those organs or tissues receiving the 3 highest values were the urinary bladder wall (124 μGy/MBq), kidneys (102 μGy/MBq), and cardiac wall (59 μGy/MBq). The mean effective dose was 26 μSv/MBq.

DISCUSSION

The purpose of this study was to evaluate the clinical safety and the whole-body biodistribution of ^{18}F after the intravenous bolus administration of ^{18}F-AH111585 in healthy adult volunteers and the associated internal radiation dosimetry. In

TABLE 1
Cumulated Activities Normalized to Administered Activity for ^{18}F-AH111585

Organ/tissue	*n**	Administered activity (MBq·h/MBq) Mean	SD
Gallbladder contents	3	0.006	0.001
Gastrointestinal tract†			
Wall	8	0.218	0.148
Small intestine contents	6	0.211	0.056
Upper large intestine contents	6	0.116	0.031
Lower large intestine contents	6	0.021	0.005
Voided feces	6	0.001	0.001
Heart			
Wall	8	0.077	0.020
Contents	8	0.043	0.006
Kidneys	8	0.155	0.031
Liver	8	0.234	0.048
Lungs	8	0.140	0.017
Salivary glands	2	0.005	0.002
Spleen	8	0.048	0.014
Thyroid gland	2	0.005	0.004
Urinary bladder contents and voided urine‡	8	0.456	0.146
Remainder	8	1.065	0.110

*Number of subjects in which organ or tissue was visualized.
†Calculated using ICRP Publication 30 (*14*) model.
‡Calculated for 3.5-h voiding interval using dynamic urinary bladder model in Stabin et al. (*15*).

TABLE 2
Organ- and Tissue-Absorbed Doses Normalized to Administered Activity for ^{18}F-AH111585

Organ/tissue	Administered activity (μGy/MBq) Mean	SD
Adrenals	15	1
Brain	6	1
Breasts	7	1
Gallbladder wall	21	4
Gastrointestinal tract		
Lower large intestine wall	23	7
Small intestine wall	44	22
Stomach wall	12	1
Upper large intestine wall	49	26
Cardiac wall	59	10
Kidneys	102	19
Liver	35	6
Lungs	30	3
Muscle	9	1
Osteogenic cells	12	1
Ovaries	17	3
Pancreas	15	1
Red marrow	10	0.5
Skin	6	1
Spleen	57	15
Testes	9	1
Thymus	10	1
Thyroid	17	21
Urinary bladder wall	124	29
Uterus	19	3

Mean effective dose per unit administered activity = 26 (±4) $\frac{\mu Sv}{MBq}$.

this study, the tracer was found to be safe and well tolerated, with 3 AEs occurring in 2 of 8 subjects. All AEs were mild and not considered to be drug-related. Washout of ^{18}F activity from the blood was rapid, with the excretion of ^{18}F being predominantly renal, resulting in the urinary bladder wall and kidneys receiving the highest absorbed doses. Uptake by the liver was relatively high, with a slow washout eventually appearing in the gastrointestinal tract.

The effective dose per unit administered activity, 26 μSv/MBq, is slightly higher than that for ^{18}F-FDG, which was recalculated in ICRP Publication 80 (*18*) as 19 μSv/MBq. For example, the effective dose of a 370-MBq administered activity (typical of many PET tracers) of ^{18}F-AH111585 is 9.6 mSv, and the absorbed dose received by the critical organ (the urinary bladder wall) would be 46 mGy. These are within the limits specified in Code of Federal Regulations 21, part 361, of 30 mSv and 50 mGy, respectively, for a single administration of radioactive material for research use.

CONCLUSION

^{18}F-AH111585 is a safe PET tracer, with a radiation dosimetry favorable for clinical PET. The effective dose is 26 μSv/MBq, which is within the range of other common ^{18}F PET imaging tracers.

ACKNOWLEDGMENTS

We thank David Turton, Adil Al-Nahhas, Sian Thomas, Andy Blyth, Andreanna Williams, James Anscombe, Hope McDevitt, Lisa Pretorius, Anne-Kirsti Aksnes, Derek Tobin, Karin Staudacher, and Kari Lyseng for their support of the trial.

REFERENCES

1. Cox D, Aoki T, Seki J, Motoyama Y, Yoshida K. The pharmacology of integrins. *Med Res Rev.* 1994;14:192–228.
2. Brooks PC. Role of integrins in angiogenesis. *Eur J Cancer.* 1996;32: 2423–2429.
3. Dredge K, Dalgeish AG, Marriott JB. Recent developments in antiangiogenic therapies. *Expert Opin Biol Ther.* 2002;2:953–966.
4. Beer AJ, Haubner R, Goebel M, et al. Biodistribution and pharmacokinetics of the $\alpha_V\beta_3$-selective tracer ^{18}F-galacto-RGD in cancer patients. *J Nucl Med.* 2005; 46:1333–1341.
5. Bach-Gansmo T, Danielsson R, Saracco A, et al. Integrin receptor imaging of breast cancer: a proof-of-concept study to evaluate ^{99m}Tc-NC100692. *J Nucl Med.* 2006;47:1434–1439.
6. Kenny L, Coombes RC, Oulie I, et al. Phase I trial of the positron emitting Arg-Gly-Asp (RGD) peptide radioligand ^{18}F-AH111585 in breast cancer patients. *J Nucl Med.* 2008;49:879–886.
7. Loevinger R, Budinger T, Watson E. *MIRD Primer for Absorbed Dose Calculations*. New York, NY: Society of Nuclear Medicine; 1988.
8. Indrevoll B, Kindberg GM, Solbakken M, et al. NC-100717: a versatile RGD peptide scaffold for angiogenesis imaging. *Bioorg Med Chem Lett.* 2006;16: 6190–6193.
9. Hudson HM, Larkin R. Accelerated image reconstruction using ordered subsets of projection data. *IEEE Trans Med Imaging.* 1994;13:601–609.
10. Defrise M, Kinahan PE, Michel CJ. Image reconstruction algorithms in PET. In: Bailey DL, Townsend DW, Valk PE, et al., eds. *Positron Emission Tomography: Basic Sciences*. London, U.K.: Springer-Verlag; 2003:91–114.
11. *ICRP Publication 89: Basic Anatomical and Physiological Data for Use in Radiological Protection: Reference Values, 89*. Oxford, England: Elsevier; 2003.
12. International Commission on Radiological Protection. *Limits for Intakes of Radionuclides by Workers*. ICRP Publication 30, Part 1. Annals of the ICRP, 2(3/ 4). Oxford, England: Pergamon Press; 1979.
13. Cloutier RJ, Smith SA, Watson EE, Snyder WS, Warner GG. Dose to the fetus from radionuclides in the bladder. *Health Phys.* 1973;25:147–161.
14. International Commission on Radiological Protection. *Age-Dependent Doses to Members of the General Public from Intake of Radionuclides*. Publication 56, Part 2. Oxford, England: Pergamon Press; 1992.
15. Stabin MG, Sparks RB, Crewe E. OLINDA/EXM: the second generation personal computer software for internal dose assessment in nuclear medicine. *J Nucl Med.* 2005;46:1023–1027.
16. International Commission on Radiological Protection. *Recommendations of the International Commission on Radiological Protection*. Publication 60. Oxford, England: Pergamon Press; 1991.
17. International Commission on Radiological Protection. *Annual Limits of Intake by Radionuclides by Workers Based on the 1990 Recommendations*. Publication 61. Oxford, England: Pergamon Press; 1991.
18. International Commission on Radiological Protection. *Radiation Dose to Patients from Radiopharmaceuticals, Addendum 2 to ICRP Publication 53*. Publication 80. Oxford, England: Pergamon Press; 1998.